Prospective Comparison of ^{18}F-FDG PET with Conventional Imaging Modalities (MRI, CT, and ^{67}Ga Scintigraphy) in Assessment of Combined Intraarterial Chemotherapy and Radiotherapy for Head and Neck Carcinoma

Yoshimasa Kitagawa, DDS, PhD[1]; Sadahiko Nishizawa, MD, PhD[2]; Kazuo Sano, DDS, PhD[1]; Toshiyuki Ogasawara, DDS, PhD[1]; Mikiko Nakamura, DDS[1]; Norihiro Sadato, MD, PhD[2]; Masanori Yoshida, MD, PhD[3]; and Yoshiharu Yonekura, MD, PhD[2]

[1]Department of Dentistry and Oral Surgery, Fukui Medical University, Fukui, Japan; [2]Biomedical Imaging Research Center, Fukui Medical University, Fukui, Japan; and [3]Department of Radiology, Fukui Medical University, Fukui, Japan

To preserve the oral organs and functions in patients with head and neck carcinoma, accurate determination of the appropriate treatment after neoadjuvant chemotherapy and radiotherapy is of critical importance. We evaluated the diagnostic accuracy of ^{18}F-FDG PET relative to that of other conventional imaging modalities in the assessment of therapeutic response after combined intraarterial chemotherapy and radiotherapy as an organ preservation protocol. **Methods:** The study was prospectively performed on 23 consecutive patients with head and neck squamous cell carcinoma who completed the treatment regimen and underwent 2 ^{18}F-FDG PET studies before and after neoadjuvant chemoradiotherapy. ^{67}Ga scintigraphy (only before therapy) as well as MRI and CT (both before and after therapy) were also performed. All images were blindly and independently interpreted without knowledge of histologic findings. The level of confidence in image interpretation was graded by means of a 5-point rating system (0 = definitely no tumor to 4 = definite tumor). **Results:** Before treatment, ^{18}F-FDG PET detected primary tumors in all 23 patients and was more sensitive (100%) than MRI (18/23; 78.3%), CT (15/22; 68.2%), and ^{67}Ga scintigraphy (8/20; 40%), with a confidence level of 3 or 4 as a positive tumor finding. After chemoradiotherapy, residual tumors were histologically confirmed in 4 patients (pathologic complete response rate, 19/23; 82.6%). Although posttreatment ^{18}F-FDG PET showed almost equal sensitivity (4/4; 100%) compared with MRI (3/3; 100%) or CT (3/4; 75%), its specificity (17/19; 89.5%) was superior to MRI (7/17, 41.2%) and to CT (10/17; 58.8%) for primary lesions. Regarding metastases to neck lymph nodes, only specificity for posttreatment images was calculated because no metastasis was confirmed in any patients after treatment. Six subjects had ^{18}F-FDG PET–positive lymph nodes, which had pathologically no tumor cells and suggested an inflammatory reactive change after therapy. Therefore, the specificity of posttreatment ^{18}F-FDG PET (17/23; 73.9%) was almost identical to that of MRI (17/20; 85%) and CT (16/21; 76.2%) for neck metastasis. With combined chemoradiotherapy monitored with ^{18}F-FDG PET, 8 patients avoided surgery and the remaining 15 patients underwent a reduced form of surgery. **Conclusion:** ^{18}F-FDG PET facilitates differentiation of residual tumors from treatment-related changes after chemoradiotherapy, which may be occasionally difficult to characterize by anatomic images. ^{18}F-FDG PET has a clinical impact for the management of patients with head and neck cancers after neoadjuvant chemoradiotherapy by optimizing surgical treatment for each patient and contributes to the improvement of the patient's quality of life.

Key Words: PET; head and neck cancer; chemotherapy; radiotherapy; organ preservation

J Nucl Med 2003; 44:198–206

In the treatment of resectable head and neck cancer, preservation of organs and functions such as speech, swallowing, and mastication as well as cosmetic appearance is of critical importance. To reduce functional damage caused by surgery, neoadjuvant chemotherapy and radiotherapy have become a primary treatment for head and neck cancer (*1–5*). Hence, precise determination of the most effective anticancer therapies before surgery is of great importance in clinical decision making regarding individual patients. Previously, the effect of anticancer treatment has been evaluated mainly on the basis of the morphologic changes that are imaged using CT and MRI. Because the size of the tumor after therapy is not directly related to the viability of the tumor, these imaging techniques have limitations in assessing therapeutic effects. In addition, neoadjuvant chemora-

Received Apr. 26, 2002; revision accepted Sep. 17, 2002.

For correspondence or reprints contact: Yoshimasa Kitagawa, DDS, PhD, Department of Dentistry and Oral Surgery, Fukui Medical University, Matsuoka, Fukui 910-1193, Japan.

E-mail: ykitagaw@fmsrsa.fukui-med.ac.jp

diotherapy can produce severe mucositis, edema, scarring, and granulation tissue, which might interfere with the detection of persistent disease using conventional diagnostic methods.

PET using ^{18}F-FDG has been confirmed to be a noninvasive, reliable diagnostic imaging tool for various kinds of malignancies, including head and neck cancers, allowing for a functional assessment of the tumor (*6*,*7*). FDG is a glucose analog, and accumulation of FDG in the cells is proportional to glucose consumption. Increased uptake of FDG, associated with increased glycolytic activity in cancer cells, can be imaged and quantified by means of PET (*8*,*9*). ^{18}F-FDG PET has an advantage over other imaging modalities to detect the change of glucose metabolism that is closely related to the viability of cancer cells.

We have previously shown the clinical value of ^{18}F-FDG PET for monitoring response to combined intraarterial chemotherapy with radiotherapy (*4*). The purpose of this study was to compare the diagnostic accuracy of ^{18}F-FDG PET with that of other conventional imaging modalities (CT, MRI, and ^{67}Ga scintigraphy) before and after combined intraarterial chemotherapy and radiotherapy as an organ preservation protocol for the management of head and neck cancer.

MATERIALS AND METHODS

Patients

The study was prospectively performed on 23 consecutive patients with head and neck cancer (18 men, 5 women; mean age, 63.8 y; age range, 47–85 y), who completed the treatment regimen described below and underwent 2 ^{18}F-FDG PET studies before and after treatment (Table 1). The clinical staging was based on the International Union Against Cancer TNM classification (*10*) and the American Joint Committee on Cancer TNM classification (*11*). The ^{18}F-FDG PET study was performed on all patients before biopsy to eliminate the influence of biopsy on PET results. Thirteen of 23 patients were in stage III or stage IV. Seventeen patients had a well-differentiated squamous cell carcinoma (SCC) and the remaining 6 patients had a moderately differentiated SCC. The study protocol was approved by the Ethical Committee of Fukui Medical University, and all patients gave written informed consent.

All 23 patients received our neoadjuvant chemoradiotherapy as an organ preservation protocol, which consisted of 2 courses of intraarterial chemotherapy, including tetrahydropyranyl adriamicin, 5-fluorouracil, and carboplatin, combined with radiotherapy (30–40 Gy) (*4*). In 7 subjects with advanced tumors crossing the midline, the catheter was placed bilaterally.

All patients underwent serial ^{18}F-FDG PET just before and >4 wk (mean, 38 d) after the combined chemoradiotherapy. As for the

TABLE 1
Patient Characteristics and Imaging Results Evaluated for Primary Tumors Before Treatment

Patient no.	Age (y)	Sex	Location	TNM	Pre-SUV*	Interpretation confidence rating			
						^{67}Ga scintigraphy	CT	MRI	PET
1	63	F	Tongue	T4 N2b M0	7.85	0	4	4	4
2	85	F	Tongue	T2 N0 M0	4.17	0	0	0	4
3	71	M	Tongue	T2 N0 M0	10.56	0	0	0	4
4	50	M	Tongue	T4 N1 M0	14.12	3	4	4	4
5	63	M	Floor of mouth	T2 N0 M1†	5.92	4	4	4	4
6	66	M	Buccal mucosa	T3 N2b M0	5.07	3	4	4	4
7	70	M	Maxillary gingiva	T2 N0 M0	7.96	0	4	3	4
8	73	F	Maxillary gingiva	rT1 N0 M0	5.29	1	3	3	4
9	71	F	Tongue	T2 N0 M0	4.07	0	0	3	4
10	47	M	Lower lip	T2 N1 M0	11.22	0	1	2	4
11	51	M	Mandible	T4 N1 M0	7.28	3	4	4	4
12	66	M	Tongue	T2 N0 M0	5.15	0	1	2	3
13	48	M	Mandibular gingiva	T2 N1 M0	7.70	4	2	2	4
14	74	M	Floor of mouth	T3 N1 M0	14.54	4	4	4	4
15	60	M	Mandibular gingiva	T4 N2a M0	12.77	3	4	4	4
16	68	M	Palatal mucosa	T1 N0 M0	9.76	0	—	3	4
17	63	M	Buccal mucosa	T3 N0 M0	5.59	0	0	3	4
18	51	F	Tongue	T2 N0 M0	8.54	0	4	4	4
19	64	M	Mandibular gingiva	T4 N0 M0	8.40	3	4	3	4
20	71	M	Floor of mouth	T2 N0 M0	6.60	—	3	3	4
21	58	M	Mandibular gingiva	T4 N0 M0	11.34	—	4	4	4
22	56	M	Floor of mouth	T4 N0 M0	26.10	0	4	3	4
23	78	M	Floor of mouth	T2 N0 M0	10.46	—	3	3	4
Average score						1.4	2.8	3.0	4.0

*Pre-SUV = pretreatment standardized uptake value.
†Lung metastasis.
Grading system: grade 0 = definitely no tumor; grade 1 = probably no tumor; grade 2 = equivocal; grade 3 = probable tumor; grade 4 = definite tumor.

conventional imaging modalities, MRI (before, $n = 23$; after, $n = 20$) and CT (before, $n = 22$; after, $n = 21$) were performed before and after treatment. In addition, ^{67}Ga scintigraphy was done in 20 patients before treatment. All examinations, including biopsies, were performed within 2 wk of each PET study.

After the second PET study following neoadjuvant chemoradiotherapy, therapeutic effects were evaluated histologically using surgical or biopsy specimens and classified as pathologic complete response ([PCR] no viable tumor cells) or as residual disease (residual tumor cells) for the primary site.

^{18}F-FDG PET

All PET imaging procedures in this study were exactly the same as in our previous study (*4*). FDG was produced using an automated FDG synthesis system (NKK, Tokyo, Japan) using a small cyclotron (OSCAR3; Oxford Instruments, Oxon, U.K.) (*12*). PET scanning was performed using an Advance system (General Electric Medical Systems, Milwaukee, WI) (*13*). Transmission scans were obtained for 10 min using a standard rod source of ^{68}Ge/^{68}Ga for attenuation correction of the emission images.

The subjects, in a fasting state, were administered 244–488 MBq (6.6–13.2 mCi) ^{18}F-FDG from the cubital vein over 10 s. In 5 patients, static images were obtained for 20 min, starting at 40 min after injection. Eighteen patients underwent dynamic PET scanning for 60 min. For these patients, we added dynamic frames from 40 to 60 min after injection to generate static images that were used for the analysis of this study. Plasma glucose levels were measured in all patients.

Conventional Imaging

CT scans were obtained using a standard CT scanner (HiSpeed Advantage RP; GE Yokogawa Medical Systems, Tokyo, Japan). We obtained contiguous transaxial images from the thoracic inlet to the base of the skull at 4- to 5-mm intervals with a slice thickness of 4–5 mm. All patients underwent both plain and contrast-enhanced scanning using 100 mL contrast material (iopamidol, 300 mg/mL; Daiichi Seiyaku, Tokyo, Japan) injected intravenously.

MR images were obtained using a 1.5-T superconducting MRI scanner (Signa 1.5T; GE Yokogawa Medical Systems). All MR studies included fast spin echo T1- and T2-weighted images. Contrast-enhanced images were obtained after an intravenous injection of Gd-diethylenetriamine pentaacetic acid (0.1 mmol/kg). In addition, postcontrast fat-suppression T1-weighted images were obtained using a presaturation pulse technique using chemical-shift selective sequence (*14*). The same fat-suppression technique was used for the fast spin echo T2-weighted images. Transaxial, coronal, and sagittal images were obtained.

Whole-body planar ^{67}Ga images were obtained using a dual-head gamma camera (RC-2500IV; Hitachi, Tokyo, Japan) 48 h after an injection of 111 MBq ^{67}Ga citrate.

Image Analysis

Three experienced examiners visually and semiquantitatively interpreted pre- and posttreatment ^{18}F-FDG PET, CT, and MRI as well as pretreatment ^{67}Ga scintigraphy independently. At the time of image interpretation, relevant correlative information concerning the histopathologic findings was not available. To compare the diagnostic accuracy of ^{18}F-FDG PET with that of the other conventional imaging modalities, these images were carefully evaluated for the detection and delineation of the primary lesions and metastases to regional lymph nodes. A level of confidence in image interpretation was graded by using a 5-point grading system (0 = definitely no tumor, 1 = probably no tumor, 2 = equivocal, 3 = probable tumor, 4 = definite tumor). For each image, we adopted the median of the grading scale values assigned by the 3 readers. In this study, we defined the confidence level of 3 and 4 as a positive tumor finding.

Finally, the results of pre- and posttreatment images for primary lesions were correlated with those of the histologic evaluation, which served as the gold standard. For regional lymph nodes, only posttreatment images were evaluated because there was no histologic confirmation of metastasis before treatment. Final diagnosis for the presence or absence of metastases to lymph nodes after chemoradiotherapy was obtained by the histopathologic findings from surgical specimens or through the follow-up of the clinical course for >1 y.

For quantitative evaluation, regions of interest (round in shape and 5 mm in diameter) were placed over the area of highest ^{18}F-FDG uptake in the tumor on the static images. The ^{18}F-FDG uptake value was corrected for the injected dose and patient body weight to obtain the standardized uptake value (SUV).

Statistical analysis was performed using the Wilcoxon signed rank test and paired Student *t* test (2-tailed). $P < 0.05$ was considered to be statistically significant. The confidence interval for a proportion was calculated according to the Wilson procedure with a correction for continuity (*15*).

RESULTS

Pretreatment Images

All pretreatment ^{18}F-FDG PET images demonstrated a focus of high ^{18}F-FDG uptake corresponding to the known primary tumor. On the basis of the 5-point grading system, ^{18}F-FDG PET was assigned to grade 4 in 22 of 23 tumors (Table 1). The average grade for ^{18}F-FDG PET (3.96) was significantly higher than that for MRI (3.0), CT (2.77), and ^{67}Ga scintigraphy (1.4). Moreover, ^{18}F-FDG PET detected small superficial tumors on the tongue, lower lip, or mandibular gingiva in 5 patients that were not detected by MRI, CT, or ^{67}Ga scintigraphy (Fig. 1).

When we consider the confidence level of 3 and 4 as a positive tumor finding, ^{18}F-FDG PET is more sensitive (sensitivity, 23/23; 100%) than MRI (18/23; 78.3%), CT (15/22; 68.2%), or ^{67}Ga scintigraphy (8/20; 40%) in detecting pretreatment primary head and neck cancer (Table 2).

Posttreatment Images and Histologic Findings for Primary Lesions

After chemoradiotherapy, all primary lesions showed an obvious decrease in size not only on visual inspection but also on CT and MRI. The histologic evaluation revealed PCR in 19 of 23 patients (PCR rate, 82.6%) without viable tumor cell in any section, which was confirmed by the fact that no patient developed a local recurrence in >3 y. The remaining 4 patients had residual tumor cells (Table 3).

Regarding the posttreatment images of the primary lesions in the 4 patients with residual tumor, the average grades for ^{18}F-FDG PET, MRI, and CT were 3.25, 3.0, and 3.0, respectively. Therefore, ^{18}F-FDG PET had an equal sensitivity (4/4; 100%) compared with that of MRI (3/3; 100%) or CT (3/4; 75%). However, the specificity of post-

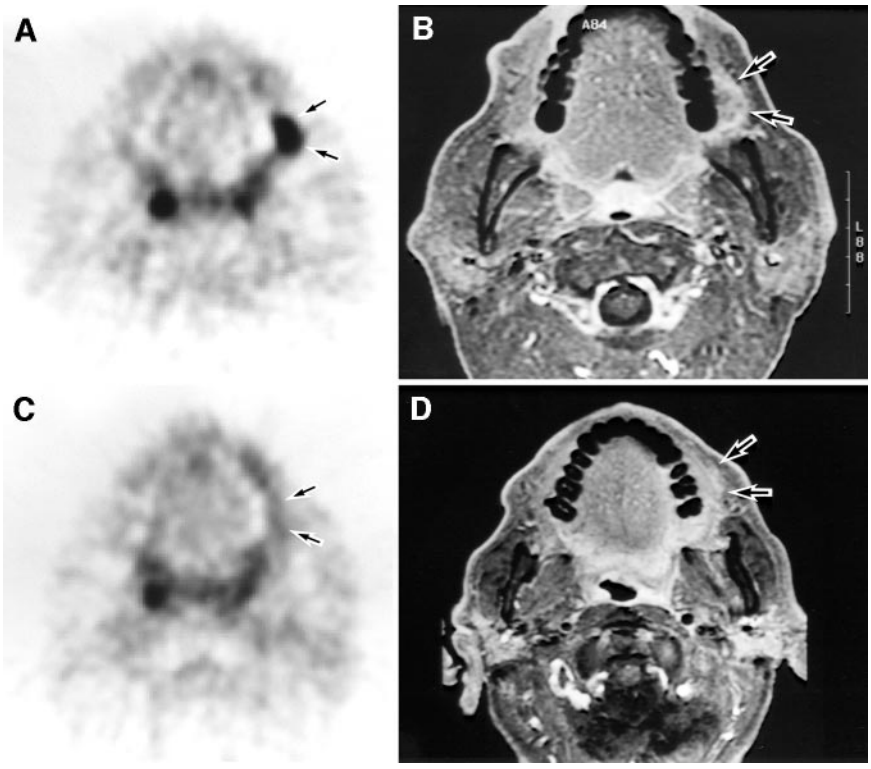

FIGURE 1. Pretreatment and posttreatment ^{18}F-FDG PET (A and C) and corresponding MR (B and D) images of 63-y-old man with squamous cell carcinoma on left buccal mucosa. (A) ^{18}F-FDG PET image shows intense focal accumulation of ^{18}F-FDG (SUV = 5.59 mg/mL) in tumor before therapy (arrows). (B) Tumor is also visualized on postcontrast fat-suppression T1-weighted MR image (B) but not on CT image. (C) After chemoradiotherapy, ^{18}F-FDG PET image reveals normalization of ^{18}F-FDG uptake (arrows; SUV = 2.80 mg/mL), consistent with histologic finding of no viable tumor cells (PCR). (D) MR image still shows contrast enhancement in tumor although it is reduced in size (arrows), which may suggest residual tumor (false-positive). On basis of PET findings, patient avoided surgery. He has remained tumor free for >4 y.

treatment ^{18}F-FDG PET (17/19; 89.5%) was superior to that of MRI (7/17; 41.2%) and CT (10/17; 58.8%) (Table 4; Figs. 1 and 2).

Posttreatment Images for Neck Lymph Nodes

Posttreatment images showed positive finding in 6 of 23 patients for ^{18}F-FDG PET, 3 of 20 for MRI, and 5 of 21 for CT, although no metastasis to neck lymph nodes was confirmed pathologically. Therefore, the specificity of posttreatment ^{18}F-FDG PET (17/23; 73.9%) was almost identical to that of MRI (17/20; 85%) or CT (16/21; 76.2%) for the neck region (Table 4). Although 8 patients showed positive findings for metastases to lymph nodes before treatment, 7 of them showed no focal ^{18}F-FDG uptake after treatment. Five of 6 patients with a focal ^{18}F-FDG uptake in the neck region after treatment did not have any focal abnormality before treatment. Although these findings were assigned as false-positive, a focal ^{18}F-FDG uptake seemed to be caused by an inflammatory reactive change after treatment (Fig. 3). There was no recurrence in neck lymph nodes for the follow-up period of >3 y. In 2 of 6 patients, no metastasis was pathologically confirmed in specimens obtained by neck dissection.

TABLE 2
Sensitivity of Pretreatment Images for Primary Tumors

Pretreatment images	^{67}Ga scintigraphy	CT	MRI	PET
True-positive (*n*)	8	15	18	23
False-negative (*n*)	12	7	5	0
Sensitivity (%)	40	68	78	100
95% CI* (%)	20–64	45–85	56–92	82–100

*95% Confidence interval (*15*).

^{18}F-FDG Findings and Further Treatment

The mean SUV for the primary tumors significantly decreased from 9.15 ± 4.79 mg/mL (range, 4.07–26.10 mg/mL) to 3.60 ± 1.55 mg/mL (range, 1.12–8.32 mg/mL) ($P < 0.01$). Lesions with residual tumor cells had a posttreatment SUV of 5.54 ± 1.63 mg/mL, whereas those without tumor cells had an SUV of 3.19 ± 1.15 mg/mL. There were no viable tumor cells in the lesion with a posttreatment SUV of <4 mg/mL. With this cutoff level of ^{18}F-FDG PET after combined chemoradiotherapy, 8 patients avoided surgery and the remaining 15 patients underwent a reduced form of surgery. No local recurrence was observed at a maximum follow-up of 7 y (mean, 4 y 4 mo; range, 3–7 y) except for 1 patient (rT1 N0 M0), who died of local recurrence (survival period, 3 y 10 mo). Three patients died of distant metastasis (survival periods, 1, 1, and 6 y) and 1 patient died of pneumonia (survival period, 1 y). The remaining 18 patients (78.2%) now survive free of cancer. The 3-y survival rate was 87%.

DISCUSSION

The clinical utility of ^{18}F-FDG PET has been well established in the detection and staging of head and neck cancers (*6*,*7*). However, few studies have reported the sensitivity of ^{18}F-FDG PET in detecting malignant tumors compared with

TABLE 3
Histologic Findings and Imaging Results Evaluated for Primary Tumors and Lymph Nodes After Treatment

Patient no.	Histologic evaluation for primary tumors after chemoradiotherapy	Post-SUV*	Interpretation confidence rating for images after chemoradiotherapy					
			CT (primary)	MRI (primary)	PET (primary)	CT (LN)	MRI (LN)	PET (LN)
1	RD	4.41	3	—	3	2	—	2
2	PCR	4.84	—	—	1	—	—	2
3	PCR	3.16	1	0	1	2	2	3
4	RD	4.39	2	3	3	1	2	0
5	PCR	4.90	4	3	3	3	2	3
6	PCR	4.25	1	4	1	2	3	4
7	PCR	2.76	3	2	0	1	1	0
8	PCR	4.77	3	3	3	2	1	1
9	PCR	1.81	2	2	0	0	0	0
10	PCR	1.12	0	1	0	2	1	0
11	RD	5.02	4	3	3	3	2	0
12	PCR	2.87	—	—	1	—	—	1
13	PCR	3.52	2	3	0	2	2	2
14	PCR	2.80	3	3	1	2	2	2
15	PCR	3.11	3	3	2	3	3	2
16	PCR	3.80	0	0	0	2	1	0
17	PCR	2.80	1	3	0	2	1	0
18	RD	8.32	3	3	4	3	3	3
19	PCR	3.53	4	3	1	0	1	3
20	PCR	1.61	1	1	1	1	0	0
21	PCR	2.76	4	3	0	3	1	1
22	PCR	4.61	2	3	0	2	2	0
23	PCR	1.56	0	1	0	2	1	3

*Post-SUV = posttreatment SUV.
LN = lymph nodes; RD = residual disease.
Grading system: grade 0 = definitely no tumor; grade 1 = probably no tumor; grade 2 = equivocal; grade 3 = probable tumor; grade 4 = definite tumor.

that of conventional diagnostic modalities—for example, functional images, such as ^{67}Ga and bone scintigraphy, as well as anatomic images, such as CT and MRI. Our study demonstrated that ^{18}F-FDG PET was more sensitive (sensitivity, 100%) with a high confidence level (grade 4, $n = 22$; grade 3, $n = 1$) than was MRI (78.3%), CT (68.2%), and ^{67}Ga scintigraphy (40%) in detecting pretreatment primary tumors of the head and neck region, probably because of the high metabolic activity of the tumor (*16,17*). Previous reports (*18–21*) showed that ^{18}F-FDG PET had a higher sensitivity (range, 78%–100%) than did CT and MRI (57%–82%), which is in agreement with our data.

Both ^{67}Ga and bone scintigraphy have been widely used for detection of distant or bone metastases as well as primary tumors. Although ^{67}Ga scintigraphy detected relatively large primary tumors in 8 of 20 patients, evaluation of tumor extent was not possible. We did not perform ^{67}Ga SPECT, although it would improve the diagnostic accuracy.

TABLE 4
Sensitivity and Specificity of Posttreatment Images for Primary Tumors and Lymph Nodes

Parameter	CT (primary)	MRI (primary)	PET (primary)	CT (LN)	MRI (LN)	PET (LN)
True-positive (*n*)	3	3	4			
False-negative (*n*)	1	0	0			
True-negative (*n*)	10	7	17	16	17	17
False-positive (*n*)	7	10	2	5	3	6
Sensitivity (%)	75	100	100			
95% CI* (%)	22–99	31–100	40–100			
Specificity (%)	59	41	89	76	85	74
95% CI* (%)	33–81	19–67	65–98	52–91	61–96	51–89

*95% Confidence interval (*15*).
LN = lymph nodes.

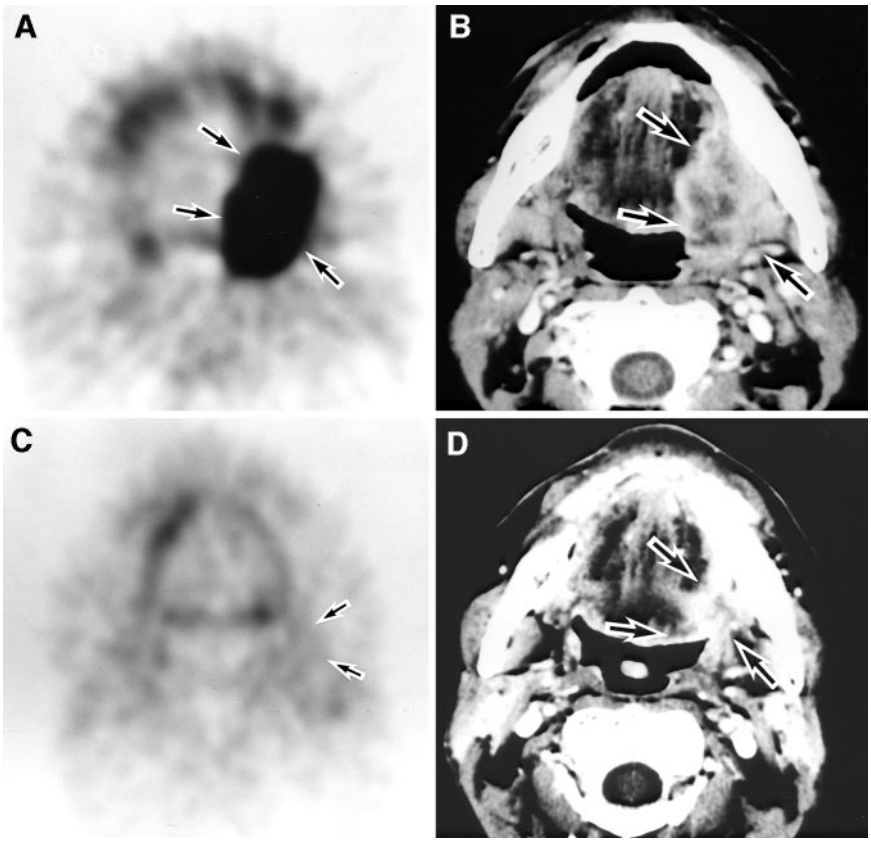

FIGURE 2. Pretreatment (A and B) and posttreatment (C and D) images of 60-y-old man with large squamous cell carcinoma (T4 N2a M0) on left mandibular gingiva. Pretreatment ^{18}F-FDG PET image (A) shows focus of high ^{18}F-FDG accumulation (SUV = 12.77 mg/mL) on left mandible (arrows), consistent with postcontrast CT (arrows, B) findings. After chemoradiotherapy, tumor disappeared on visual inspection with slight induration. (C) Posttreatment ^{18}F-FDG PET image shows no abnormal ^{18}F-FDG accumulation (arrows; SUV = 3.11 mg/mL), consistent with histologic finding (PCR). (D) CT image shows remarkable reduction in tumor size but does not exclude residual tumor because of contrast enhancement (arrows). According to ^{18}F-FDG PET findings, patient successfully underwent functional neck dissection and marginal resection of mandible, requiring neither continuous resection of mandible nor reconstructive surgery.

In contrast, ^{18}F-FDG PET clearly visualized the tumor extent that fully corresponded to CT or MRI findings. Furthermore, ^{18}F-FDG PET detected small tumors that were not detected by CT or MRI but were apparent by visual inspection. As for the whole-body evaluation, we have previously shown that whole-body ^{18}F-FDG PET images had a clinical impact on the management of patients with head and neck cancer by reliably detecting secondary primary malignancies as well as distant metastases (*22*). ^{18}F-FDG PET with whole-body imaging would replace the conventional functional imaging modalities of ^{67}Ga and bone scintigraphy.

^{18}F-FDG PET has been used to monitor response to therapies in patients with head and neck cancers (*4,23–30*). To our knowledge, however, no report has described prospectively the diagnostic value of ^{18}F-FDG PET in patients with head and neck cancer as a functional imaging modality in comparison with CT and MRI as morphologic modalities before and after treatment with a consistent regimen of combined intraarterial chemotherapy and radiotherapy as an organ preservation protocol. Four of 23 patients demonstrated residual tumors after the therapy. ^{18}F-FDG PET had almost equal sensitivity (4/4; 100%) compared with CT (3/4; 75%) or MRI (3/3; 100%). However, in the remaining 19 patients with no viable tumor cells, the specificity of posttreatment ^{18}F-FDG PET (17/19; 89.5%) was superior to that of CT (58.8%) and MRI (41.2%). A high false-positive rate was shown on posttreatment CT (7/17) and MRI (10/17). Therefore, CT or MRI does not reliably differentiate posttreatment tissue changes from the residual tumor. The floor of the mouth, the parapharyngeal space, the base of the tongue, and the cheek were the areas that were particularly difficult to assess using anatomic images because posttreatment fibrosis, diffuse edematous swelling, and granulation tissue demonstrated such contrast enhancement that we could not differentiate the persistent residual tumor. This will be a problem especially when we make a decision regarding further treatment on the basis of anatomic images after chemoradiotherapy. ^{18}F-FDG PET correctly identified residual tumors independent of their size and site and was also superior to anatomic imaging modalities in excluding residual tumors. We concluded that increased ^{18}F-FDG uptake on PET images obtained >4 wk after treatment strongly indicated the presence of residual tumor, whereas the absence of ^{18}F-FDG uptake suggested that no viable tumor remained.

Assessment for possible metastases to the neck lymph nodes is important in determining further treatment for each patient. Precise assessment of the neck region may avoid unnecessary surgery in patients without metastases to lymph nodes. Several studies (*31–34*) showed that ^{18}F-FDG PET detected metastases to neck lymph nodes at a high sensitivity (range, 72%–91%) and specificity (82%–99%) in patients with head and neck carcinoma. But these patients underwent neither chemotherapy nor radiotherapy preoperatively, which might affect ^{18}F-FDG uptake in the tumor. In our study, neck lymph nodes were histopathologically eval-

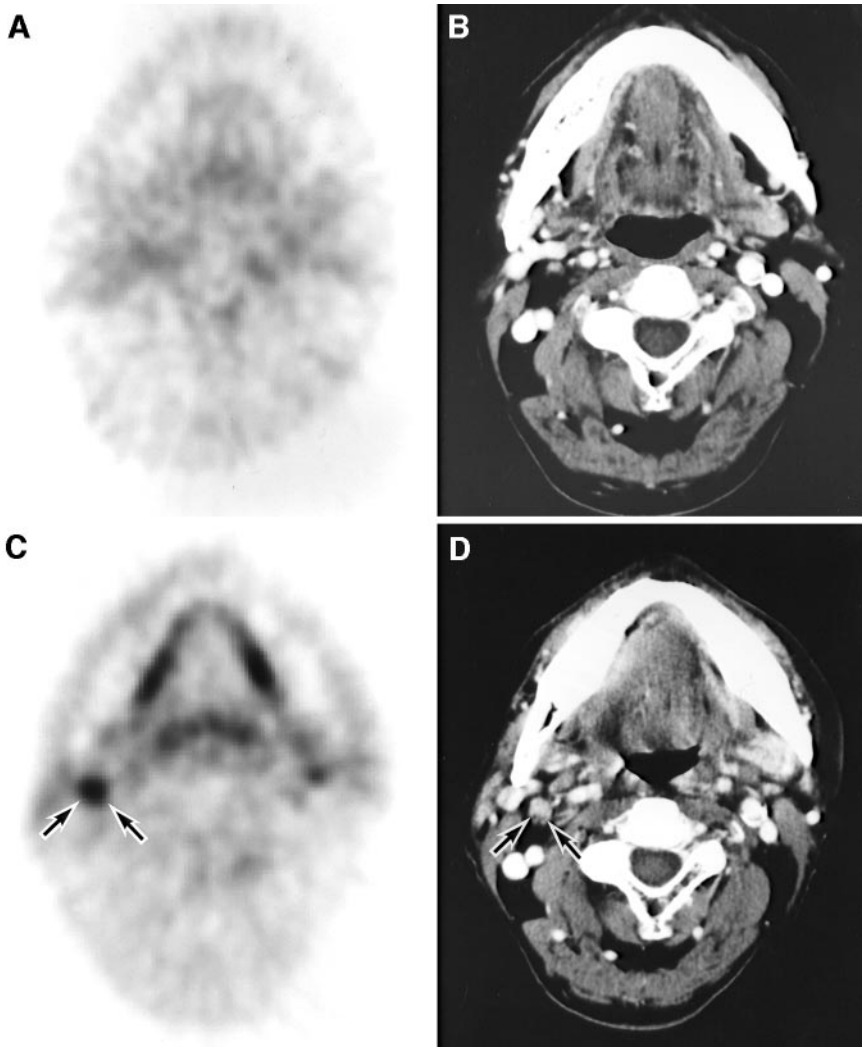

FIGURE 3. Pretreatment (A and B) and posttreatment (C and D) neck images of 78-y-old man with squamous cell carcinoma (T2 N0 M0) on floor of mouth. Pretreatment PET (A) and corresponding postcontrast CT (B) images demonstrate no metastasis to neck lymph nodes. (C) After chemoradiotherapy, neck lymph nodes were not palpable and posttreatment PET image shows abnormal ^{18}F-FDG uptake in neck region (arrows, false-positive) probably due to inflammatory and reactive change. (D) Posttreatment CT image shows small lymph node (<1 cm; arrows, true-negative) in neck region, suggesting no metastasis. Patient was confirmed to have no metastasis in neck by clinical follow-up for >3 y.

uated after combined intraarterial chemotherapy and radiotherapy, and no metastasis was confirmed in any patients, including 8 patients with suspected N (+) status by the pretreatment evaluation with imaging modalities. This finding may indicate the efficacy of our organ preservation regimen in treatment of metastases to the neck lymph nodes as well as the primary tumor (PCR rate, 82.6%). This is probably due to the high concentration of anticancer drugs in neck lymph nodes provided by intraarterial chemotherapy, together with concomitant neck irradiation. However, ^{18}F-FDG PET after treatment demonstrated a focal ^{18}F-FDG uptake in the neck region of 6 patients, which was assigned as a false-positive finding. For the primary lesions, there were only 2 false-positive cases after therapy. As a result, specificity of posttreatment ^{18}F-FDG PET (17/23; 73.9%) was not better than that of MRI (17/20; 85%) or CT (16/21; 76.2%) for the neck region (Table 4). A focal ^{18}F-FDG uptake in these patients was probably attributable to the reactive or inflammatory process in the neck lymph nodes, which might persist for a longer period than that in primary sites after intraarterial chemoradiotherapy. Follow-up ^{18}F-FDG PET 3 mo after therapy showed no abnormal uptake in the neck of patients with false-positive findings and there was no recurrence in neck lymph nodes for >3 y.

The use of functional information obtained by ^{18}F-FDG PET for therapeutic planning is promising. Familiarity with the complex anatomy of the head and neck is essential for accurate interpretation of ^{18}F-FDG PET images because functional images alone often do not provide sufficiently detailed anatomic information describing the surrounding normal structures that is necessary for therapeutic planning. Although ^{18}F-FDG PET provides information not available by means of MRI or CT, it cannot replace these anatomic modalities. In our facility, image coregistration between ^{18}F-FDG PET and CT or MRI has been available recently and has been used clinically in selected cases (*35*). We conclude that serial ^{18}F-FDG PET and MR or CT images are essential for the management of head and neck cancer treated by an organ preservation protocol such as combined intraarterial chemotherapy and radiotherapy.

Precise evaluation of the presence or absence of residual viable tumor is particularly important to the preservation of

oral organs and functions by avoiding surgery or performing a reduced form of surgery after neoadjuvant chemoradiotherapy. In our previous study, we showed the significance of quantitative analysis of ^{18}F-FDG PET in patients with head and neck cancer before and after the same intraarterial chemotherapy and radiotherapy (*4*). The SUV before the therapy is useful for predicting the response to the treatment, whereas the SUV after the therapy is useful for diagnosing the presence or absence of residual tumor. This study confirmed these findings regarding the SUV and further indicated the significance of the diagnostic values of ^{18}F-FDG PET by comparing it with anatomic images. We attempted to determine further treatment on the basis of the ^{18}F-FDG PET data. In 8 patients assigned a complete response with posttreatment SUVs of <4.0, we were able to avoid surgery. The remaining 15 patients underwent a reduced form of surgery with clinical advantages of a lower risk of damaging esthetics and a greater preservation of oral functions. The follow-up data at 3 y after the treatment revealed no local recurrence in all patients, which confirmed the validity of our use of ^{18}F-FDG PET in determination of further treatment after neoadjuvant chemoradiotherapy. Furthermore, the 3-y survival rate was 87%. These results indicate that ^{18}F-FDG PET is a powerful tool for accurate assessment of the therapeutic effect, which is essential for planning further treatment with reducing the risk of surgery and preserving appearance and functions. In this way, ^{18}F-FDG PET can contribute to the improvement of the quality of life of patients with head and neck cancers.

CONCLUSION

Neoadjuvant intraarterial chemotherapy combined with radiotherapy is an effective presurgical treatment for reducing a risk of surgery and preserving oral functions in patients with head and neck cancer. ^{18}F-FDG PET has a clinical impact on patient management by facilitating differentiation of residual tumors from treatment-related changes after the chemoradiotherapy, which is sometimes difficult to characterize by means of anatomic images. ^{18}F-FDG PET will contribute to the improvement of the quality of life of patients with head and neck cancers by aiding in the selection of the optimal treatment option for each patient.

ACKNOWLEDGMENT

This study was supported in part by a Grant-in-Aid for Scientific Research (C11671982) from the Ministry of Education, Science, Sports and Culture, Japan.

REFERENCES

1. Adelstein DJ, Kalish LA, Adams GL, et al. Concurrent radiation therapy and chemotherapy for locally unresectable squamous cell head and neck cancer: an Eastern Cooperative Oncology Group pilot study. *J Clin Oncol.* 1993;11:2136–2142.
2. Dragovic J, Doyle TJ, Tilchen EJ, et al. Accelerated fractionation radiotherapy and concomitant chemotherapy in patients with stage IV inoperable head and neck cancer. *Cancer.* 1995;76:1655–1661.
3. Benasso M, Corvo R, Numico G, et al. Concomitant administration of two standard regimens of chemotherapy and radiotherapy in advanced squamous carcinoma of the head and neck: a feasibility study. *Anticancer Res.* 1995;15:2651–2654.
4. Kitagawa Y, Sadato N, Azuma H, et al. FDG PET to evaluate combined intra-arterial chemotherapy and radiotherapy for head and neck neoplasms. *J Nucl Med.* 1999;40:1132–1137.
5. Newkirk KA, Cullen KJ, Harter KW, Picken CA, Sessions RB, Davidson BJ. Planned neck dissection for advanced primary head and neck malignancy treated with organ preservation therapy: disease control and survival outcomes. *Head Neck.* 2001;23:73–79.
6. Strauss LG, Conti PS. The applications of PET in clinical oncology. *J Nucl Med.* 1991;32:623–648.
7. Bar-Shalom R, Valdivia AY, Blaufox MD. PET imaging in oncology. *Semin Nucl Med.* 2000;30:150–185.
8. Som P, Atkins HL, Bandoypadhyay D, et al. A fluorinated glucose analog, 2-fluoro-2-deoxy-D-glucose (F-18): nontoxic tracer for rapid tumor detection. *J Nucl Med.* 1980;21:670–675.
9. Flier JS, Mueckler MM, Usher P, Lodish HF. Elevated levels of glucose transport and transporter messenger RNA are induced by ras or src oncogenes. *Science.* 1987;235:1492–1495.
10. Hermanek P, Sobin LH, eds. *UICC: TNM Classification of Malignant Tumours.* 4th ed. Berlin, Germany: Springer-Verlag; 1987:13–18.
11. Fleming ID, Cooper JS, Henson DE, et al., eds. *AJCC Cancer Staging Manual.* 5th ed. Philadelphia, PA: Lippincott Williams & Wilkins; 1997:21–31.
12. Hamacher K, Coenen HH, Stoecklin G. Efficient stereospecific synthesis of no-carrier-added 2-[^{18}F]-fluoro-2-deoxy-D-glucose using aminopolyether supported nucleophilic substitution. *J Nucl Med.* 1986;27:235–238.
13. DeGrado TR, Turkington TG, Williams JJ, et al. Performance characteristics of a whole-body PET scanner. *J Nucl Med.* 1994;35:1398–1406.
14. Kitagawa Y, Ishii Y, Kawamura Y, Hayashi K, Ogasawara T, Morihiro H. Usefulness of fat-suppression magnetic resonance imaging for oral and maxillofacial lesions. *Int J Oral Maxillofac Surg.* 1996;25:457–462.
15. Newcombe RG. Two-sided confidence intervals for the single proportion: comparison of seven methods. *Stat Med.* 1998;17:857–872.
16. Higashi K, Clavo AC, Wahl RL, et al. Does FDG uptake measure proliferative activity of human cancer cell? in vitro comparison with DNA flow cytometry and tritiated thymidine uptake. *J Nucl Med.* 1993;34:414–419.
17. Haberkorn U, Strauss LG, Reisser C, et al. Glucose uptake, perfusion and cell proliferation in head and neck tumors: relation of positron emission tomography to flow cytometry. *J Nucl Med.* 1991;32:1548–1555.
18. Rege S, Maass A, Chaiken L, et al. Use of positron emission tomography with fluorodeoxyglucose in patients with extracranial head and neck cancers. *Cancer.* 1994;73:3047–3058.
19. Laubenbacher C, Saumweber D, Wagner-Manslau C, et al. Comparison of fluorine-18-fluorodeoxyglucose PET, MRI and endoscopy for staging head and neck squamous-cell carcinomas. *J Nucl Med.* 1995;36:1747–1757.
20. Wong WL, Chevretton EB, McGurk M, et al. A prospective study of PET-FDG imaging for the assessment of head and neck squamous cell carcinoma. *Clin Otolaryngol.* 1997;22:209–214.
21. Keyes JW Jr, Watson NE Jr, Williams DW 3rd, Greven KM, McGuirt WF. FDG PET in head and neck cancer. *AJR.* 1997;169:1663–1669.
22. Kitagawa Y, Nishizawa S, Sano K, et al. Whole-body ^{18}F-fluorodeoxyglucose positron emission tomography in patients with head and neck cancer. *Oral Surg Oral Med Oral Pathol Oral Radiol Endod.* 2002;93:202–207.
23. Minn H, Paul R, Ahonen A. Evaluation of treatment response to radiotherapy in head and neck cancer with fluorine-18 fluorodeoxyglucose. *J Nucl Med.* 1988;29:1521–1525.
24. Rege SD, Chaiken L, Hoh CK, et al. Change induced by radiation therapy in FDG uptake in normal and malignant structures of the head and neck: quantitation with PET. *Radiology.* 1993;189:807–812.
25. Haberkorn U, Strauss LG, Dimitrakopoulou A, et al. Fluorodeoxyglucose imaging of advanced head and neck cancer after chemotherapy. *J Nucl Med.* 1993;34:12–17.
26. Greven KM, Williams DW, Keyes JW Jr, et al. Positron emission tomography of patients with head and neck carcinoma before and after high dose irradiation. *Cancer.* 1994;74:1355–1359.
27. Berlangieri SU, Brizel DM, Scher RL, et al. Pilot study of positron emission tomography in patients with advanced head and neck cancer receiving radiotherapy and chemotherapy. *Head Neck.* 1994;16:340–346.
28. Lowe VJ, Dunphy FR, Varvares M, et al. Evaluation of chemotherapy response

in patients with advanced head and neck cancer using [F-18]fluorodeoxyglucose positron emission tomography. *Head Neck.* 1997;19:666–674.
29. Dalsaso TA, Lowe VJ, Dunphy FR, Martin DS, Boyd JH, Stack BC. FDG-PET and CT in evaluation of chemotherapy in advanced head and neck cancer. *Clin Positron Imaging.* 2000;3:1–5.
30. Hubner KF, Thie JA, Smith GT, Chan AC, Fernandez PS, McCoy JM. Clinical utility of FDG-PET in detecting head and neck tumors: a comparison of diagnostic methods and modalities. *Clin Positron Imaging.* 2000;3:7–16.
31. Braams JW, Pruim J, Freling NJ, et al. Detection of lymph node metastases of squamous-cell cancer of the head and neck with FDG-PET and MRI. *J Nucl Med.* 1995;36:211–216.
32. McGuirt WF, Williams DW 3rd, Keyes JW Jr, et al. A comparative diagnostic study of head and neck nodal metastases using positron emission tomography. *Laryngoscope.* 1995;105:373–375.
33. Benchaou M, Lehmann W, Slosman DO, et al. The role of FDG-PET in the preoperative assessment of N-staging in head and neck cancer. *Acta Otolaryngol.* 1996;116:332–335.
34. Adams S, Baum RP, Stuckensen T, Bitter K, Hor G. Prospective comparison of ^{18}F-FDG PET with conventional imaging modalities (CT, MRI, US) in lymph node staging of head and neck cancer. *Eur J Nucl Med.* 1998;25:1255–1260.
35. Uematsu H, Sadato N, Yonekura Y, et al. Coregistration of FDG PET and MRI of the head and neck using normal distribution of FDG. *J Nucl Med.* 1998;39:2121–2127.

JNM The Journal of NUCLEAR MEDICINE

Prospective Comparison of ^{18}F-FDG PET with Conventional Imaging Modalities (MRI, CT, and ^{67}Ga Scintigraphy) in Assessment of Combined Intraarterial Chemotherapy and Radiotherapy for Head and Neck Carcinoma

Yoshimasa Kitagawa, Sadahiko Nishizawa, Kazuo Sano, Toshiyuki Ogasawara, Mikiko Nakamura, Norihiro Sadato, Masanori Yoshida and Yoshiharu Yonekura

J Nucl Med. 2003;44:198-206.

The Journal of Nuclear Medicine is published monthly.
SNMMI | Society of Nuclear Medicine and Molecular Imaging
1850 Samuel Morse Drive, Reston, VA 20190.
(Print ISSN: 0161-5505, Online ISSN: 2159-662X)

SNMMI SOCIETY OF NUCLEAR MEDICINE AND MOLECULAR IMAGING